Single Photoionization of Radon (Z = 86)

Santosh Kumar

Research Scholar,
Department of Physics,
B. R. A. Bihar University, Muzaffarpur-842001,

Abstract : We performed the time-dependent linear response approximation within the framework of the relativistic density functional method (DFM) the self-consistent calculation for Radon and computed total cross-section for the photon energy range 7-28 eV. The large difference between the results obtained from IPA-model and the present time-dependent response model is clearly seen from the graph. The large peak due to the ionization from $6p_{1/2} \rightarrow d_{3/2}$ in the IPA-model is marked significantly due to polarization effect incorporated in the time-dependent response model.

IndexTerms - Photoionization, cross section, wave function, atom.

I. INTRODUCTION

Calculation of photoionization cross-sections of atoms and ions are useful in a variety of investigations in plasma physics ,atomic physics and flashlamp photopumping schemes for x-ray lasers. The existing calculations of photoionization cross-sections using the single electron or the independent particle model (IPM) ,the energy-levels, and wavefunctions of the atom or ion are first calculated using the Hartree-Fock (HF) method. The interaction of the incident electromagnetic radiation with the atom (or ion) is treated via the first order perturbation theory. For many electron atoms and ions with a large number of bound electrons, substantial discrepancies are found between experimental and IPM-data [1].

Here, we used the time-dependent linear response approximation within the framework of the relativistic density functional method (DFM) [2, 3, 4] to treat the problem of photoionization. This method incorporates certain advantages over the HF-method. In the density functional method, one deals with a set of local equations only that leads to computational simplicity and fairly accurate atomic energy levels, wave functions, etc. are obtained. The computational simplicity is even more apparent in the case of relativistic DFM verses relativistic HF-methods. In the DFM, correlation effects of the bound electrons in the atom are accounted for in a simple way via the correlation potential. The Hartree-Fock method, on the other hand, does not take into account electron correlation, although it accounts for non-local exchange effects appropriately.

The independent particle method does not take into account the polarization effect of the atom brought about by the incident time-varying radiation field. In the linear response method within the density functional method, this is treated adequately – as will be seen from comparison with the experimental data. In most experimental situations, the incident radiation (from synchrotron sources or lasers) have field strengths small compared to the atomic field strengths. For those experimental conditions, the present model based on linear response is adequate and useful.

Photopumping scheme for x-ray lasers, population inversion of excited ionic levels, computation of opacities of plasmas for diagnostic and target response effects require calculations of photoionization and photoexcitation cross-sections and rates data as input. Accurate calculations are necessary for interpreting experimentally available data on cross sections. So, there is a need for relativistic modeling of these processes in order to generate accurate data over a wide range of photon energy for a variety of atoms and ions. The present model provides such a tool and its usefulness will be discussed in subsequent sections.

We will present result of photoionization cross-section of atom in a dense plasma medium and examine the modification of cross-sections due to the plasma environment.

Due to the lack of experimental data, the photoionization cross sections of radon were known mainly from theoretical works.

Theoretical methods [9, 8, 10, 5,7] like MCDF, R-matrix, DFM etc, have proven to give accurate photoionization cross section data at high photon energy, far from the thresholds, but give poor results near thresholds where resonant structure. P. Quinet and co-workers reviewed the recent advances in the determination of atomic parameters for modeling K lines in cosmically abundant elements [6].This work has included the effect of radiation damping, but takes only into account the photoionization from ground state, thus neglecting any contribution from the metastable states.

II. THEORY : [METHOD OF CALCULATION]

Using the local density functional method in the first part of the calculation of energy-level spectrum and the wave functions of the particular atom of specific configuration were done. To treat many-electron atoms (with high Z) appropriately, relativistic DFM equations were used. In this method, the following set of equations were solved self-consistently:

$$\left[c\boldsymbol{\alpha}.\mathbf{p}+c^2\beta\ +u(\mathbf{r})\right]\ \psi_i(\mathbf{r})\ =\ \ E_i\,\psi_i(\mathbf{r}) \qquad \text{.....(1)}$$

$$u\ (\mathbf{r})=-\frac{Z}{r}\ +\int\frac{\rho(\mathbf{r}')\,dr'}{|\mathbf{r}-\mathbf{r}'|}+\frac{\partial}{\partial\rho(\mathbf{r})}\left[\rho(\mathbf{r})\,\varepsilon_{XC}\ \left(\rho(\mathbf{r})\right)\right] \qquad \text{.....(2)}$$

and $$\rho\ (\mathbf{r})=\sum_i f_i\left|\psi_i(\mathbf{r})\right|^2 \qquad \text{.....(3)}$$

where, $\rho(\mathbf{r})$ is the electronic charge density of the atom, $\boldsymbol{\alpha}$ and $\boldsymbol{\beta}$ are the Dirac matrices, f_i's are the integral occupation factors corresponding to the number of electrons in each state $\psi_i(\mathbf{r})$ with corresponding energy eigenvalue E_i. The atomic potential $u\ (\mathbf{r})$ contains, in addition to the nuclear and the electrostatic Hartree term, a contribution arising from the electron exchange and correlation effects. Let us note that the use of integer occupation factors f_i's for the given configuration distinguishes this model from the "average atom model" where the occupation factors are taken to be those given by the statistical Fermi distribution function.

The orbital functions are four-component spinors. They are split into major and minor components:

$$\psi(\mathbf{r})=\begin{pmatrix}\psi^1(\mathbf{r})\\ \psi^2(\mathbf{r})\end{pmatrix}=\begin{pmatrix}(A(r)/r)\ i^l\ \Omega_{jlm}(\mathbf{r})\\ (B(r)/r)\ i^l\ \Omega_{jl'm}(\mathbf{r})\end{pmatrix} \qquad \text{..... (4)}$$

where A and B are major and minor components of the radial functions and $\Omega_{jlm}(\mathbf{r})$ and $\Omega_{jl'm}(\mathbf{r})$ are two-component Pauli spinors with the indicated numbers. The various quantum numbers are related by -

$$l'=l+s,\quad j'=l+1/2,\ s=l'-1/2s,\ K=-s(j+1/2);\ s=\pm1 \qquad \text{..... (5)}$$

The differential equations for A and B (in matrix form) are:

$$\frac{d}{dr}\begin{pmatrix}A\\ B\end{pmatrix}=\begin{pmatrix}-K/r & (u-E-c^2)/cs\\ -(u-E+c^2)/cs & K/r\end{pmatrix}\begin{pmatrix}A\\ B\end{pmatrix} \qquad \text{..... (6)}$$

In equation (2), ε_{XC} is the exchange-correlation energy of the electrons. In actual calculation, Gunnarsson-Lundquist (G-L) form [3] for exchange-correlation energy and potential was used. It is well known that reliable atomic data is obtained from the use of G-L exchange-correlation. Equation (1)-(6) are solved numerically to self-consistency to obtain the wave functions ψ_i's, the binding energies of each orbital E_i, the atomic charge density $\rho(\mathbf{r})$ and the self-consistent potential $u(\mathbf{r})$.

Now consider the effect of an incident time-varying radiation field $E(t)=E_0 e^{i\omega t}$ on the atom. It induces a time-dependent atomic density deviation, $\delta\rho(\mathbf{r},t)$, causing a time-dependent polarization effect. For the linear response method used here, it is convenient to work with the Fourier transform:

$$\delta\rho(\mathbf{r},t)=\frac{1}{2\pi}\int_{-\infty}^{\infty}\delta\rho(\mathbf{r},\omega)\,e^{-i\omega t}d\omega \qquad \text{..... (7)}$$

The net induced density due to the external plus the induced potential is

$$\delta\rho_{ind}(\mathbf{r},\omega)=\int\chi(\mathbf{r},\mathbf{r}',\omega)\left[V_{ext}(\mathbf{r},\omega)+V_{ind}(\mathbf{r},\omega)\right]d\mathbf{r}' \qquad \text{..... (8)}$$

where the induced potential is given by

$$V_{ind}(\mathbf{r},\omega)=\int\frac{\delta\rho(\mathbf{r}',\omega)}{\mathbf{r}-\mathbf{r}'}d\mathbf{r}'+\frac{\partial V_{XC}(\rho(\mathbf{r}))}{\partial\rho(\mathbf{r})}\delta\rho(\mathbf{r},\omega) \qquad \text{..... (9)}$$

The response function is given by

$$\begin{aligned}\chi(\mathbf{r},\mathbf{r}',\omega)=&\sum_i f_i\psi_i^*(\mathbf{r})\,\psi_i(\mathbf{r}')\,\mathrm{G}(\mathbf{r},\mathbf{r}',E_i+\omega)\\&+\sum_i f_i\psi_i(\mathbf{r})\,\psi_i^*(\mathbf{r}')\,\mathrm{G}^*(\mathbf{r},\mathbf{r}',E_i-\omega)\end{aligned} \qquad \text{..... (10)}$$

and thus involves the wave functions and energy levels of the atoms. The Green's functions are solutions of the inhomogeneous Dirac equation

$$\left[c\boldsymbol{\alpha}.\boldsymbol{\rho}+c^2\beta+u(\mathbf{r})-E\right]\mathrm{G}(\mathbf{r},\mathbf{r}',E)=-\delta(\mathbf{r}-\mathbf{r}') \qquad \text{..... (11)}$$

In actual calculation, angular decomposition of the Green's function in terms of spherical harmonics is done and the radial part is treated separately as follows:

The Green's function G in equation (11) has 16 components, which are represented in matrix form

$$G(\mathbf{r},\mathbf{r}',E)=\begin{pmatrix}G^{11}(\mathbf{r},\mathbf{r}'|E) & G^{12}(\mathbf{r},\mathbf{r}'|E)\\ G^{21}(\mathbf{r},\mathbf{r}'|E) & G^{22}(\mathbf{r},\mathbf{r}'|E)\end{pmatrix}$$

The angular decomposition of various terms are

$$G^{11}(\mathbf{r},\mathbf{r}'|E)=\sum_{jlm}\Omega_{jlm}(\mathbf{r})\,G^{11}_{jl}(\mathbf{r},\mathbf{r}'|E)\,\Omega^N_{jlm}(\mathbf{r}')$$

$$G^{12}\left(\mathbf{r},\mathbf{r}'\middle|E\right)=\sum_{jlm} i^{l-l'}\Omega_{jlm}\left(\mathbf{r}\right)\,G^{12}_{jl}\left(\mathbf{r},\mathbf{r}',\middle|E\right)\,\Omega^{*}_{jlm}\left(\mathbf{r}'\right)$$

$$G^{21}\left(\mathbf{r},\mathbf{r}'\middle|E\right)=\sum_{jlm} i^{l'-l}\Omega_{jl'm}\left(\mathbf{r}\right)\,G^{21}_{jl}\left(\mathbf{r},\mathbf{r}',\middle|E\right)\,\Omega^{*}_{jlm}\left(\mathbf{r}'\right)$$

$$G^{22}\left(\mathbf{r},\mathbf{r}'\middle|E\right)=\sum_{jl'm}\Omega_{jl'm}\left(\mathbf{r}\right)\,G^{22}_{jl'}\left(\mathbf{r},\mathbf{r}',\middle|E\right)\,\Omega^{*}_{jl'm}\left(\mathbf{r}'\right) \qquad \text{..... (12)}$$

The radial part $G^{\alpha\beta}\left(\mathbf{r},\mathbf{r}'\middle|E\right)$ are solutions of the radial inhomogeneous Dirac equation

$$G^{\alpha\beta}_{jl}\left(\mathbf{r},\mathbf{r}'\middle|E\right)=\begin{cases}\mathrm{v}^{\alpha}_{jl}\left(r\right)\mathrm{v}^{\beta}_{jl}\left(r'\right)/\left(rr'W_{jl}\right) & r<r'\\ \mathrm{v}^{\alpha}_{jl}\left(r\right)\mathrm{v}^{\beta}_{jl}\left(r'\right)/\left(rr'W_{jl}\right) & r>r'\end{cases} \qquad \text{..... (13)}$$

W_{jl} is the Wronskian

$$W_{jl}=eS_{jl}\left[\mathrm{v}^{2}_{jl}\left(r\right)\,\bar{\mathrm{v}}^{1}_{jl}\left(r\right)-\bar{\mathrm{v}}^{2}_{jl}\left(r\right)\,\mathrm{v}^{1}_{jl}\left(r\right)\right]=\text{ const.}$$

$\bar{\mathrm{v}}^{1}_{jl}\left(r\right)$ and $\bar{\mathrm{v}}^{2}_{jl}\left(r\right)$ are major and minor component radial functions that are real and regular at r = 0. $\bar{\mathrm{v}}^{1}_{jl}\left(r\right)$ and $\bar{\mathrm{v}}^{2}_{jl}\left(r\right)$ major and minor comment radial functions which (for E > c^2) are complex and obey outgoing wave boundary conditions at r = ∞. The phase for $\bar{\mathrm{v}}^{1}_{jl}$ and $\bar{\mathrm{v}}^{2}_{jl}$ are real and decay exponentially at large radii.

With the above representations, the polarizability $\chi\left(\mathbf{r},\mathbf{r}',\omega\right)$ is given by

$$\chi_{j}\left(\mathbf{r},\mathbf{r}',\omega\right)=\sum f_{i}\left(2j_{2}+1\right)\left(2l_{1}+1\right)\left(2l_{2}+1\right)\left[\begin{pmatrix}l_{1} & l_{2} & \bar{l}\\ 0 & 0 & 0\end{pmatrix}\begin{pmatrix}\bar{l} & l_{1} & l_{2}\\ 1/2 & j_{2} & j_{1}\end{pmatrix}\right]^{2}$$

$$\frac{1}{W_{j_2l_2}\left(E_i\pm\omega\right)}\left[A_{i}\left(r\right)\,\mathrm{v}^{1}_{\mathrm{j}_2l_2}\left(r\middle|\varepsilon_i\pm\omega\right)\pm i^{S_1-S_2}B_{i}\left(r\right)\,\mathrm{v}^{2}_{\mathrm{j}_2l_2}\left(r\middle|\varepsilon_i\pm\omega\right)\right]$$

$$\left[A_{i}\left(r'\right)\,\bar{\mathrm{v}}^{1}_{\mathrm{j}_2l_2}\left(r'\middle|\varepsilon_i\pm\omega\right)\pm i^{S_2-S_1}B_{i}\left(r'\right)\,\bar{\mathrm{v}}^{2}_{\mathrm{j}_2l_2}\left(r'\middle|\varepsilon_i\pm\omega\right)/\left(rr'\right)^{2}\,\middle|\,\right] \qquad \text{..... (14)}$$

when $r<r'$, and r and r' are interchanged on the right side of equation (14) when $r>r'$. The index i stands for the quantum numbers (n, l_1, j_1, s_1,) of a bound state and f_i fore the occupation factors. The summation is over all indices except I and over both + ω and – ω. For the case of –ω, the complex conjugates of all outgoing waves in equation (14) are to be used. Angular momentum coupling coefficients are expressed in terms of Wigner 3j and 6j symbols.

The frequency dependent polarizability $\boldsymbol{\alpha}\left(\omega\right)$ is the ratio of the induced dipole moment to the external field:

$$\boldsymbol{\alpha}\left(\omega\right)=-\frac{e}{E_0}\int Z\,\delta\rho\left(\mathbf{r},\omega\right)d\mathbf{r} \qquad \text{..... (15)}$$

Note that $\boldsymbol{\alpha}\left(\omega\right)$ like $\delta\rho\left(\mathbf{r},\omega\right)$ is complex. The induced density deviation (and also the corresponding induced potential) can have a phase difference with respect to that of the applied external field. Once $\boldsymbol{\alpha}\left(\omega\right)$ is determined, the photoabsorption cross-section $\sigma\left(\omega\right)$ of the atom is obtained form:

$$\sigma(\omega) = \frac{4\pi\omega}{c} \operatorname{Im}\boldsymbol{\alpha}(\omega). \quad \text{..... (16)}$$

Partial cross section for comparison with IPA -model

In order to see the connection with the IPA-model, consider the partial cross-section due to photoionization from a specific bound state $\psi_i(\mathbf{r})$ to a final continuum state $\psi_f(\mathbf{r})$.

The initial atomic state is represented as

$$\psi_i(\mathbf{r}) = \frac{U_{nl}(r)}{r} Y_L(\mathbf{r}) \quad \text{..... (17)}$$

and the final continuum state with wave function **K** and energy ε as

$$\psi_f(\mathbf{r}) = 4\pi \sum_{L'} A_{l'} i^{l'} \frac{P\varepsilon l'(r)}{r} Y^*_{L'}(\mathbf{K}) Y_{L'}(\mathbf{r}) \quad \text{..... (18)}$$

The complex coefficients A_l's are found by requiring $\psi_f(\mathbf{r})$ to behave asymptotically as an incident plane wave plus a spherical wave. Then the partial cross-section σ_{nl} is shown to be

$$\sigma_{nl}(\omega) = 2(2l+1)\alpha\,\hbar\,\omega\sqrt{\varepsilon}\,a_B^2 \sum_{L'} \left| A_l^2 \left| \langle l\ 100 | l'0 \rangle \right|^2 \right| \int P_{\varepsilon l'}(r) V^{SCF}(r,\omega) U_{nl}(r) dr \Big|^2 \quad \text{..... (19)}$$

where $\langle l\ 100 | l'0 \rangle$ is a Clebsch-Gordan coefficient.

In (19), V^{SCF} (r, ω) is a frequency dependent complex self-consistent potential. Note that, if V^{SCF} (r, ω) is replaced by the usual dipole moment operator, one obtains the conventional or independent particle approximation(IPA) result. In actual calculations, both bound and continuum wave functions are generated numerically using the Numerov method for integrating the Dirac equation. Let us also note that the real and imaginary parts of the self-consistent final contribute to the partial cross-section without interference. Computations were performed for both the conventional independent particle model and the time-dependent linear response to density functional method for comparison purposes.

III. Results & Discussion

In the time-dependent response model for Radon (Z = 86), relativistic effects are significant. So the Dirac equation approach in our model is suitable. We performed self-consistent calculation for Radon and the computed total cross-section is plotted in Fig.1 for the photon energy range 7-28 eV. The large difference between the results obtained from IPA-model and the present time-dependent response model is clearly seen from the graph. The large peak due to the ionization from $6p_{1/2} \rightarrow d_{3/2}$ in the IPA-model is masked significantly due to polarization effect incorporated in the time-dependent response model. No experimental data is available for the case of Radon. However, in view of the good agreement between experimental data and the results of time-dependent response model, it is expected that future experimental measurements for Radon in this photon energy range will be in close agreement with these calculated cross-sections.

The result presented above is for single atoms without the effect of the plasma environment – as appropriate for very low density plasmas. For high density plasmas, however, effects due to screening shifts

of energy levels, modification of wave functions of bound (particularly the upper levels) and continuum wave functions as well as potentials of the ion embedded in the plasma have to be considered.

For proper treatment these effects, the self-consistent density functional method (DFM) at finite temperatures [5] should be used. The application of this method requires iterative numerical solution of Schrödinger equation involving the complete set of bound and continuum wave functions for the multi-electron ion and construction of effective potential inclusive of plasma screening and electronic exchange correlation effect in each interaction. For our present purpose, we adopted the following simplified approach for computational simplicity. For a given plasma density and temperature, we represent the long range part of the effective potential in the Debye-screened form. The inner part of the effective potential was constructed by numerical integration of the Hartree term with the electron density distribution calculated using the bound state wave functions.

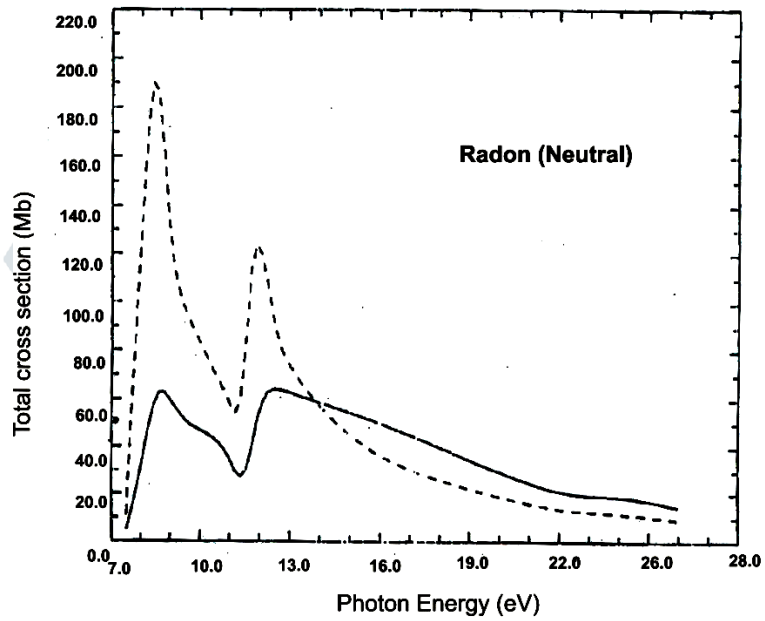

Fig.: Photoionization cross section (PICS) of Radon (Rn)

- - - - - - - Independent Particle Model (Ref.01)

——————— Time- dependent Density Functional Calculation (Present Result)

IV. CONCLUSION

It is demonstrated that the time-dependent linear response method within the framework of local relativistic density functional theory can provide reliable atomic data for various atoms and ions of experimental interest. This model is particularly useful in those situations where conventional independent particle models fail to provide accurate data. The mechanism of time-dependent polarization of the atom is seen to be important in describing the observed results. As a practical point, the computer code based on the time-dependent model is fast and efficient, capable of generating a large number of data in a short time (for example , cross-sections for 10 photon energies for a medium-Z atom takes about 3 minutes of c. p. u. times on a Cray-XMP computer). The present method is capable of treating large complex atoms with high-Z for which relativistic effects are important. Let us point out that if the applied radiation field strength is very high, so that it is comparable or larger than the atomic field strength, new extensions or developments of the present model is necessary to treat those conditions. Full numerical solution of time-dependent density functional method (beyond the linear response approximation) would be one suitable to use in those cases. Work in this direction in planned for future.

With reference to the calculations for the different plasma conditions, let us point out that the Debye-screened form for the long range part of the potential may not be adequate for the high-density plasmas. For more relativistic calculation, it is necessary to use fully self-consistent finite temperature density functional

method for those plasma conditions. Also, the effect of exchange and correlation for plasma electrons become important at high densities. The present approximate scheme is used at present for computational simplicity. However, the results shown here clearly indicate that with increasing plasma density, the photoionization cross-section and rates of the ions forming the plasma can be substantially modified. Accurate modeling of atomic properties for dense plasmas, therefore, requires that the effect of the surrounding plasma should be properly included in the calculation.

REFERENCES

[1] U. Fano and J. W. Cooper, Rev. Mod. **40**, 441 (1986).
[2] M. J. Scott and E. Zaremba, Phys. Rev. A **21**, 12 (1980).
[3] A. Zangwill and P. Soven, Phys. Rev. A **21**, 1561 (1980).
[4] D. Liberman and A. Zangwill, Comput. Phys. Commun. **32**, 75 (1984).
[5] U. Gupta, M. Blaha and J. Davis, J. Phys. B **17**, 3617 (1984).
[5] Enrico Clementi and Carla Roetti, At. Data Nucl. Data Tables **14** 177-478 (1974).
[6] M. Stener, P. Decleva, D. M. P. Holland and D. A. Shaw, J. Phys. B: At. Mol. Opt. Phys. **44** 075203 (2011).
[7] M. F. Gharaibeh, J.M.Bizau, D. Cubaynes, S. Guilbaud, N. El. Hassan, M. M. Al. Shorman, C. Miron, C. Nicolas, E. Robert, C. Blancard and B. M. McLaughlin, *J. Phys. B: At. Mol. Opt. Phys.* **44**, 175208 (2011).
[8] M. H. Chen, K. J. Reed and D. M. Mcwilliams, *Atomic data and nuclear data tables* **65**, 289-370 (1997).
[9] J. Garcıa, T. R. Kallman, M. Witthoeft, E. Behar, C. Mendoza, P. Palmeri, P. Quinet, M.A. Bautista, and M. Klapisch. *The Astrophysical Journal Supplement Series* **185**, 477-485 (2009).